

Modeling and Analysis of Voltage Source based Battery Energy Storage System in Microgrid to Improve Power Quality

Faiqa Tariq¹ and Tahir Mahmood

Electrical Engineering Department, University of Engineering and Technology, Taxila, 47050, Pakistan

¹Corresponding author: Faiqa Tariq (faiqatariq98@gmail.com).

Abstract- Rising demand of renewable energy sources based distributed generation poses several challenges in utility grid operation. These shortcomings have been solved by microgrid. Power quality improvement is the main technical challenge in the applications of microgrid. Renewable energy sources can be integrated with microgrid in a better way by introducing a battery energy storage system. Power quality improvement, voltage and frequency regulation and catering the intermittency of renewable energy sources are few advantages of battery energy storage system. Integration of voltage source-based battery energy storage system in solar photovoltaic connected microgrid is presented in this paper. Voltage level between main grid and generation of solar power is maintained with the help of battery energy storage system. Power quality improvement of integrated microgrid system is done with control strategy of bidirectional converter used in battery energy storage system. Hysteresis band current controller is used in this paper to control the currents of battery energy storage system. It is a simple as well as robust technique for reduction of total harmonic distortion and voltage profile improvement as shown in the simulation results. Total harmonic distortion of system voltage is reduced 0.20%. This paper also presents the power flow to the loads using hysteresis band current controller. It is also shown by results that 45kVA is the most feasible rating of VS to deal with both linear and non-linear loads. MATLAB/SIMULINK environment is used to model and simulate the overall system performance. Proposed control technique can be used in autonomous microgrids to fix critical disturbances in future.

Index Terms-- Battery energy storage system, microgrid, nonlinear loads, solar photovoltaic, total harmonic distortion, voltage source

I. INTRODUCTION

Management of the grid is changing from centralized schemes to decentralized schemes due to the rising trend of distributed generation (DG) in grid. This may lead to various issues that must be handled carefully for the proper operation of electrical grid. The conventional network of distribution suffers from issues of reliability, efficiency and quality [1]. The concept of microgrid (MG) is a promising solution for renewable energy sources (RES) integration as it is a weak grid on a small-scale and can operate in grid-connected mode as well as islanded-mode [2]. Several advantages are offered by MG for example, utilizing RES that are environmentally friendly and lower financial responsibility as compared to wholesome power generation [3]. Furthermore, distribution networks have also become more reliable with the introduction of MG, as transmission network interruptions didn't affect sensitive loads. In a nutshell, deployment of MG can help in achieving valuable goals such as saving of cost, lower carbon emission and reliability [4]. On the other hand, various technical and regulatory issues are still faced by MG systems. Requirements of landscape, uncompetitive electricity market and regulated pricing of government are included in regulatory issues, whereas stability issues of dynamic system, protection relaying

coordination and Power quality (PQ) are the main technical issues. Hence, MGs have become more popular in recent years due to the above-mentioned advantages. PQ and stability related issues may be caused with the penetration of RES due to their stochastic nature [5]. Use of RES is increased due to various reasons regarding economic aspects, environmental issues and policies of government.

Solar energy sources are being used effectively in varied hybrid power systems, as illustrated in Fig. 1 amongst all developed RES [6, 7]. Solar photovoltaic (PV) systems have lately received much interest from utility companies worldwide [8]. Although this renewable energy production is localized in a few geographic places around the country, it cannot be called marginal generation, and substantial consideration must be paid to balancing its fluctuation. There is an achievable target to boost renewable power; therefore, figuring away ahead intended for easing large-scale integration of such RES while maintaining grid security in mind is critical. Power safety has become a significant concern, with more renewable energy being generated and more nonlinear loads. Battery energy storage systems (BESS) is used to overcome the issues of stability due to dynamic nature of RESs as they cause voltage sags and swells [9-11].

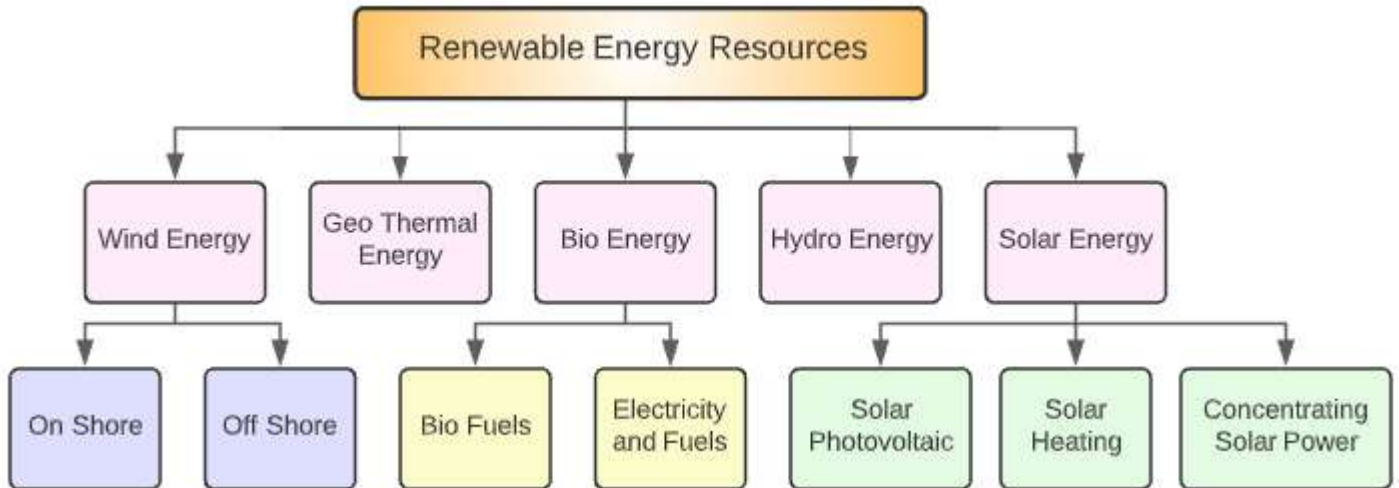


FIGURE 1. Classification of Renewable Energy Resources

In the literature, various control strategies based on energy storage have been demonstrated. In [12], it was proposed that technique of Fuzzy logic controller is used to control BESS based MG system. Dynamic response of the proposed controller was much better than classical PID controller. In [13], control strategy of BESS was proposed based on active and reactive power to restore voltage and frequency of MG during contingencies. Conventional microgeneration, Fuel Cell (FC), PV and wind turbine (WT) system was included in MG system. An adaptive neuro-fuzzy algorithm was employed by author to tune controller gains. In [14-17], other control techniques to enhance dynamic response of system was proposed during abnormal conditions. Dynamic performance of these control methods was good but, complex calculations were involved in them and power quality was also not improved significantly by them [18-20]. Therefore, these techniques are not highly recommended.

Owing to the above-mentioned discussion, hysteresis band current control (HBCC) based novel control technique of BESS under normal and abnormal conditions is presented in this paper. It is a very good and easy technique to compare the reference current (I_{ref}) with the current of inverter's output known as actual current (I_0). Switching signals of inverter is generated in the result of this comparison in order to get quick response. In this way, a band is created around I_{ref} known as hysteresis band. I_{ref} is generated by using inverse park transformation which is also known as dq0 to ABC transformation. Power quality improvement is the main technical issues regarding MG applications as mentioned earlier and different unknown disturbances are subjected due to this issue. Hence, this problem can be solved with the use of innovative HBCC based control technique [21]. Voltage and frequency must be maintained at point of common coupling (PCC) within specified limits to improve MG's power quality. Furthermore, it is also shown by several investigations that a certain number of harmonics, variation in power factor (PF) and current unbalancing are added into PCC to the grid by connecting RES and nonlinear loads [22]. Sinusoidal pattern of voltage source (VS) is altered due to nonlinear load by introducing frequency distortions into the

power grid. Voltage and current outputs will be distorted at PCC by interlinking power electronic devices-based loads with grid. As a result, production of heat is increased and efficiency and lifespan of VS is also affected [23].

This paper mainly focusses on the following objectives:

- To control the three-phase currents of BESS with the help of HBCC to improve power quality of MG
- To investigate the technoeconomic size of VS by incorporating different non-linear loads in the network
- To perform FFT analysis with HBCC and without HBCC to shown the reduction in total harmonic distortion (THD)

The rest of the paper is structured as: system model is presented in section 2. Section 3 illustrates modeling of solar farm. The next section 4 describes the comprehensive modeling of proposed BESS and its control system. In section 5, results and discussions are illustrated. Finally, section 6 concludes the whole discussion.

II. SYSTEM MODEL

The details of proposed MG system are presented in this section. PV array is connected at DC link in MG system under consideration. After that, PV array connected with the main power grid that is modelled as three-phase voltage source with the rating of 400V. The ac side frequency and voltage are maintained at 50 Hz and 400V (line to line), respectively. Another local VS such as uninterruptable power supply (UPS) is also connected to the system for transient conditions when there will be no renewable source. Fig. 2 shows the detailed model of the MG system under consideration. Table 2. illustrates the complete specifications of the proposed MG system.

Local VS is implemented as three-phase programmable VS block in Simulink while executing the simulation. The BESS is also connected at PCC through an inverter to offer an extra support of active power (P) and reactive power (Q) for the MG system. Both critical loads and non-critical loads of single-phase as well as three-phase are included in the system. The MG system is operated in two modes; grid-connected mode and islanded mode. A three-phase circuit breaker is used to disconnect the main grid from the rest of the network.

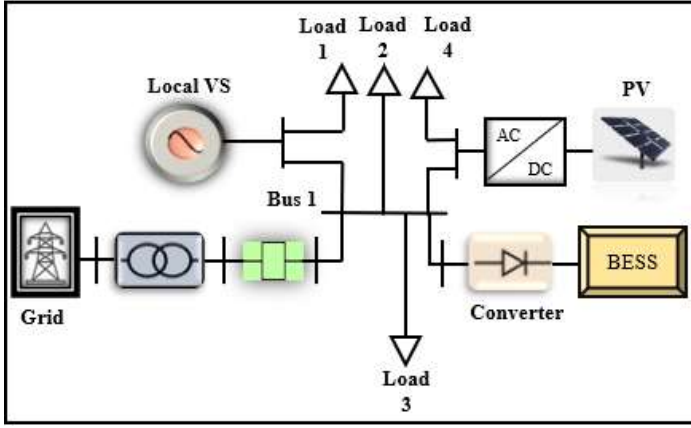


FIGURE 2. Model of proposed microgrid system
TABLE I
SPECIFICATIONS OF MICROGRID SYSTEM

S. No	Source/Load Type	Specification
1	Main Grid Rating	400 V, 50 Hz, 500 kVA
2	BESS Rating	100 kW and 50kWh
3	Local VS	3-phase 400 V, 50 Hz
4	Solar Photovoltaic	100 kW
5	Three-phase Load	6.45 kVA, 0.93 PF
6	Single-phase Load	Ph-1: 12kVA, 0.80 PF Ph-2: 14.3kVA, 0.6 PF Ph-3: 3.5kVA, 0.67 PF

III. SOLAR SYSTEM MODELING

Basically, it is fundamental element of solar system. Direct current (DC) is generated when light falls on solar cell [24, 25]. The relationship between solar irradiance and generated DC current is linear. Fig. 3 shows the equivalent circuit of PV cell. A diode and a resistance are present in parallel with an ideal current source in cell along with a series resistance. The characteristics of voltage and current of solar cells are described by the following equations:

$$I = I_L - I_0 \left(e^{\frac{q(V+IR_S)}{KT}} - 1 \right) - \frac{V+IR_S}{R_{Sh}} \quad (1)$$

V and I represents output voltage and current of cell, I_L and I_0 denote light generated current and saturation current of diode, respectively in (1). q is the electron charge. R_S and R_{Sh} denotes the series resistance and parallel resistance. K and T denotes Boltzmann constant and temperature (Kelvin), respectively. This equation is only valid when the value of ideality factor will be 1 and named as single diode model.

$$I_L = \left(\frac{Y}{Y_{ref}} \right) [I_{L,ref} + C_T(T - T_{ref})] \quad (2)$$

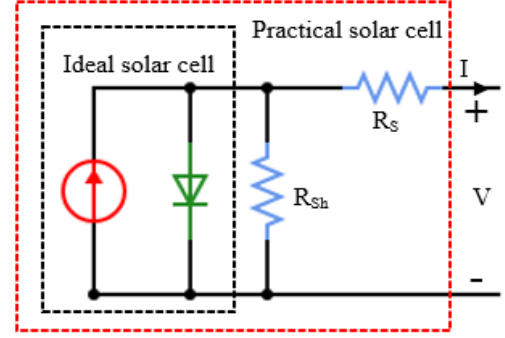


FIGURE 3. Equivalent circuit of solar cell

In (2), solar irradiance is denoted by Y , whereas C_T shows the coefficient of temperature.

$$I = N_p I_L - N_p I_0 \left(e^{q \left(\frac{V+IR_S}{N_p+N_s} \right) \frac{1}{KT}} - 1 \right) - \frac{N_p}{R_{Sh}} \left(\frac{V}{N_s} + \frac{IR_S}{N_p} \right) \quad (3)$$

Number of cells connected in series and parallel are represented as N_s and N_p in (3). Maximum Power Point Tracking (MPPT) of solar panels is performed by Perturb & Optimization (P&O) algorithm [26]. The tracking speed and accuracy of PV array is improved by this method. A function block is used for MPPT algorithm. Boost converter steps up the voltage to the higher value which is then converted to the AC voltage with the help of a Voltage Source Inverter (VSI) [27]. P-V and I-V Plot of PV array is presented in Fig. 4 [28]. The photovoltaic system is illustrated in Fig. 5. Parameters of PV array used for the performance of paper is as follows: Temperature=298K, irradiance=1000w/m², open circuit voltage=65V, short circuit current=6A.

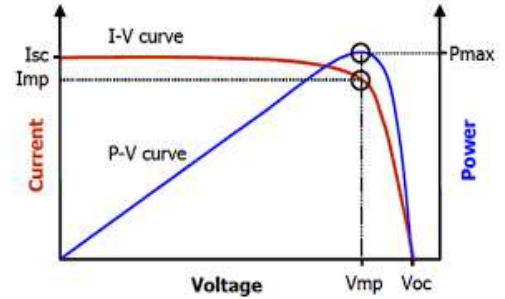


FIGURE 4. Solar cell P-V and I-V characteristics [28]

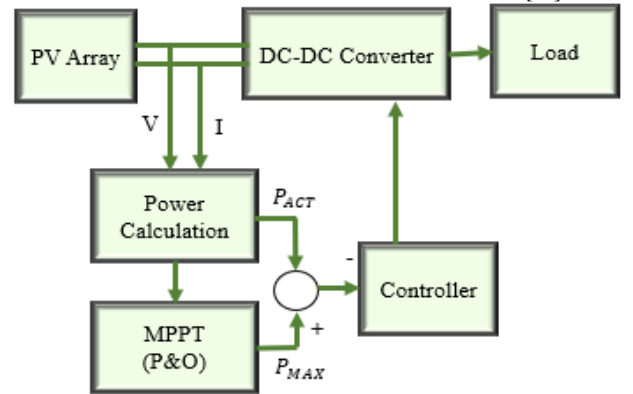


FIGURE 5. Block diagram of solar system

IV. BESS MODEL AND ITS CONTROL SYSTEM

BESS acts as energy buffer to feed all loads individually under certain conditions to achieve specific goals and it is placed within distribution subsystem [9]. Mostly, all the loads are fed by grid directly, and battery is also charged by the grid at the same time when excess energy is available [29]. Excess energy is supplied to the loads when consumption is more. When the supply of grid is interrupted, BESS supports the microgrid temporarily as emergency backup power [30]. Model of BESS consists of two main parts, a DC source and a voltage source inverter (VSI) as shown in Fig. 6. DC source is the main “Battery storage block” of BESS, VSI is used to integrate the DC source with PCC. A filter is also provided at the input and output side of BESS [31].

Currents of BESS in both d and q-axis are described by the two equations given below, respectively;

$$\frac{di_d}{dt} = \frac{-\omega_0 R_{VSI}}{L_{VSI}} i_d + \frac{\omega}{\omega_0} i_q + \frac{\omega_0}{L_{VSI}} (mV_{DC} \cos(\theta + \varphi) - V_d) \quad (4)$$

$$\frac{di_q}{dt} = \frac{-\omega_0 R_{VSI}}{L_{VSI}} i_q + \frac{\omega}{\omega_0} i_d + \frac{\omega_0}{L_{VSI}} (mV_{DC} \sin(\theta + \varphi) - V_q) \quad (5)$$

where, R_{VSI} and L_{VSI} is the resistance and inductance of VSI. V_{DC} indicates the voltage of DC link capacitor, whereas m and φ is the VSI modulation index and phase angle, respectively. ω_0 and ω are the reference frequency and system frequency. The voltage of DC link capacitor is:

$$\frac{dV_{DC}}{dt} = \frac{m}{C_{DC}} (i_q \cos(\varphi) + i_d \sin(\varphi)) + \frac{V_{battery} - V_{DC}}{R_{battery} C_{DC}} \quad (6)$$

In (6), C_{DC} denotes the capacitance of DC-link. $R_{battery}$ is the resistance of battery or DC source.

A. HYSTERESIS BAND CURRENT CONTROLLER

Essentially, this is a robust technique of feedback current control. Reference current (I_{ref}) is followed by the actual current through the branch of BESS inside the defined upper and lower limits hysteresis band. Reference current is generated by the controller by sensing the V_{DC} across capacitor and ac terminal voltage in the inverter’s dc side. Load current’s reactive component starts increasing with the increase in reactive component of load power [32]. The magnitude of I_q component of I_{ref} is obtained by sensing the rise in reactive current. After sensing V_{DC} across capacitor and compared with the value set as reference. The magnitude of I_d component of I_{ref} is obtained by passing the signal of error through PI controller. Actual signals of currents and reference currents for BESS are compared by a comparator.

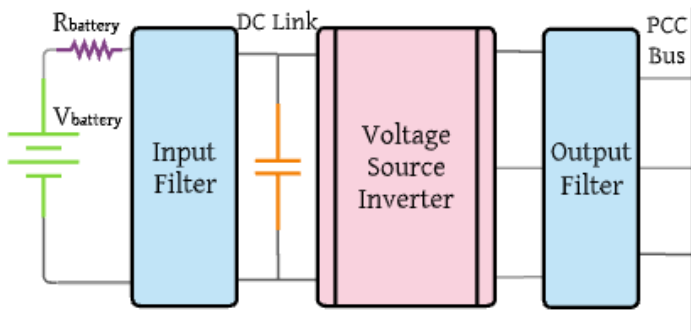


FIGURE 6. Block diagram of battery energy storage system

Then, gate signals are generated for the multiple times switching of switch pairs in inverter leg per cycle so that the I_{ref} must be followed by the actual current of inverter within the defined hysteresis band limits [33]. Current waveform through the branch of inverter, I_{ref} for a phase and switching instants are shown in Fig. 7 [32]. The controller generates the lagging I_{ref} consumed by the load, given as:

$$I_{ref} = I_m \sin(\omega t - 90^\circ - \theta^\circ) \quad (7)$$

where:

$$I_m = \sqrt{I_d^2 + I_q^2} \quad (8)$$

$(-90^\circ - \theta^\circ)$ = Angle of lag I_{ref} of concerning VS

The current upper and lower band limits are described as:

$$I_{ref(upper)} = I_m \sin(\omega t - 90^\circ - \theta^\circ) + HB \quad (9)$$

$$I_{ref(lower)} = I_m \sin(\omega t - 90^\circ - \theta^\circ) - HB \quad (10)$$

Relay output will be one when difference between I_{ref} and I_0 will be less than or equal to -0.5 . Similarly, Relay output will be zero when difference between I_{ref} and I_0 will be greater than or equal to $+0.5$.

B. INVERSE PARK TRANSFORMATION

In the proposed technique, dq0 to ABC transformation is used to generate reference current signals of BESS. Another name of dq0 to ABC transformation is Inverse Park Transformation [34, 35].

$$\begin{bmatrix} \mu_a \\ \mu_b \\ \mu_c \end{bmatrix} = \begin{bmatrix} \cos(\theta) & -\sin(\theta) & 1 \\ \cos(\theta - \frac{2\pi}{3}) & -\sin(\theta - \frac{2\pi}{3}) & 1 \\ \cos(\theta + \frac{2\pi}{3}) & -\sin(\theta + \frac{2\pi}{3}) & 1 \end{bmatrix} \begin{bmatrix} \mu_d \\ \mu_q \\ \mu_0 \end{bmatrix} \quad (11)$$

V. RESULTS AND DISCUSSION

Power flow during transient time and steady state period is performed by executing the simulation for three different events; 1st event is when grid is connected to the system, 2nd scheme is when grid is out and VS is supplying power, and in last event, BESS is ramped up and fed all the loads. During the above-mentioned three events, power required by loads, power supplied by VS and BESS considering nonlinearity and current unbalancing is shown in Table 2. VS kVA rating varies between 35-45 kVA. In transient time-interval, 140-190 % of overload capabilities should be possessed to handle the loads. It is also observed that the uniform balanced current is supplied by BESS through all three-phases after ramping up completely.

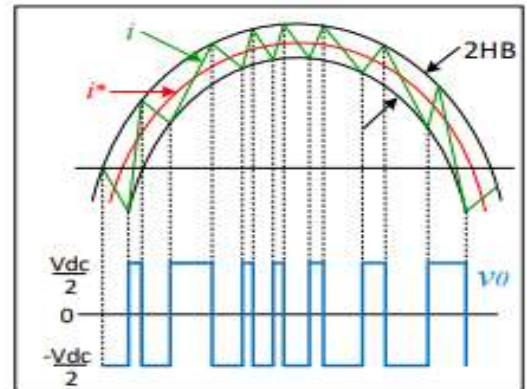


FIGURE 7. Switching patterns and Controller waveform [32]

TABLE II
EFFECT OF CURRENT UNBALANCING AND NONLINEARITY ON
POWER SUPPLIED BY VS AND BESS

S. No	Non linearity (%)	Current Unbalancing (%)	Power Fed by VS (kVA)	Power Fed by BESS (kVA)	Power of the Loads (kVA)
1	6.8	3.2	35.7	76.8	93
2	17	10.9	40.1	85.6	100
3	10.5	5.1	37.9	77.4	97.3
4	5	14.5	37.44	66.5	84.5
5	21.02	15	42.67	92	108.1
6	23.01	16.98	44.59	96	110
7	17.2	11.1	39	70.9	89

A. ACTIVE AND REACTIVE POWER BY VS, BESS AND LOAD
Active and reactive power of load is 6000W and 2400kVAR respectively. Active and reactive power fed by VS and BESS is given in Fig. 8(a) and 8(b), respectively.

B. VOLTAGE ACROSS THE CAPACITOR
In this system, source itself provide the active power losses in the branch of BESS. Therefore, only reactive power is provided by capacitor. Voltage across capacitor must be a constant value. In this case, the value of voltage across capacitor is 600V.

C. COMPARISON OF PROPOSED TECHNIQUE WITH PREVIOUS TECHNIQUE USING FFT ANALYSIS

THD an essential feature for evaluating harmonics level in waveforms of system voltage and current, could also be used to describe power quality under various load situations, in contrast to the fundamental waveforms of the system voltages and currents. Intermittent nature of RES and nonlinear loads cause harmonics in the system. FFT analysis is performed for harmonics investigation using MATLAB-Simulink. THD of system voltage without applying proposed control strategy and with control system is 30% and 0.20% tool and shown in Fig. 9(a) and 9(b), respectively and it is according to the specified limits in standard IEEE 519-119.

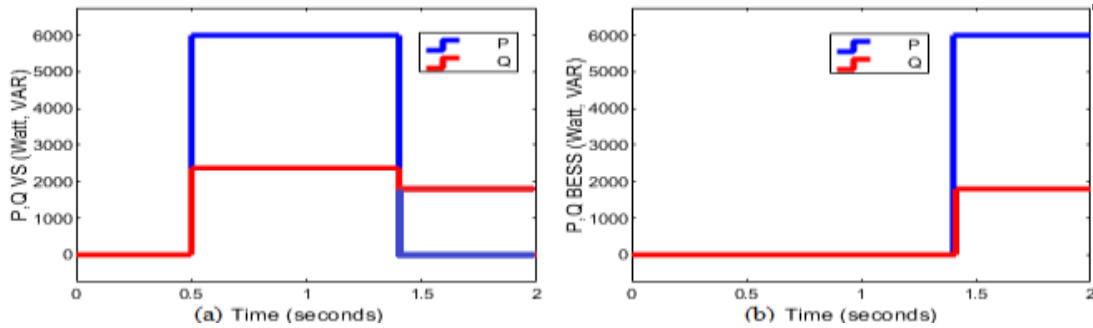


FIGURE 8. Power by VS, BESS. (a) Active and reactive power fed by VS, (b) Active and reactive power given by BESS

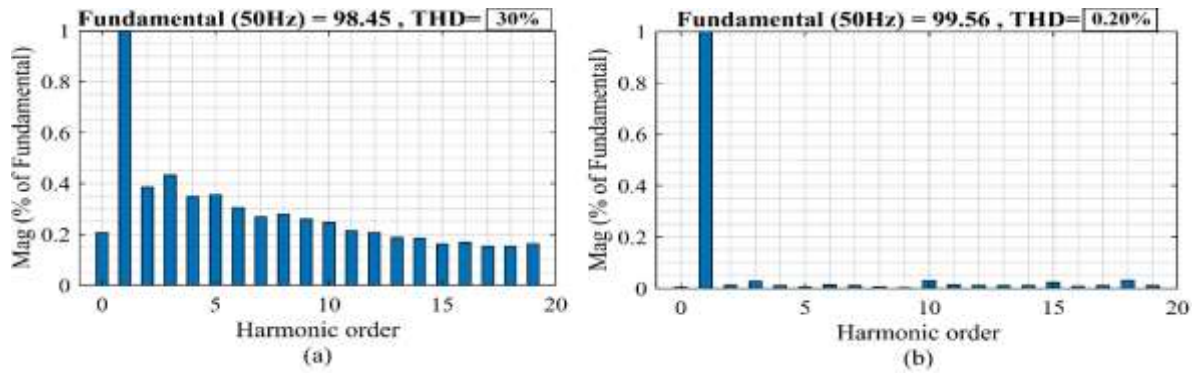


FIGURE 9. FFT Analysis for Comparison. (a) Harmonics without HBCC [32], (b) Harmonics with HBCC

VI. CONCLUSION

PV and an effective coordinated control of battery energy storage system is presented in this work for power quality improvement of microgrid system. Performance of hysteresis band current controller-based system is investigated by running a simulation

into MATLAB-Simulink using different loads. In this paper, Effect of current unbalancing and nonlinearity is also taken into consideration. An effective control is shown by HBCC over BESS operation. Simulation results clearly presented that THD is 0.20% with the proposed technique and 30% without using proposed technique. Moreover, voltage is also regulated at 1pu at load bus

during normal and transient conditions and make this system more reliable. 45 kVA is the most feasible rating of VS as shown by simulation results. For future work, proposed control technique can be used in autonomous microgrids to fix critical disturbances.

REFERENCES

- [1] F. H. Gandoman *et al.*, "Review of FACTS technologies and applications for power quality in smart grids with renewable energy systems," *Renewable and sustainable energy reviews*, vol. 82, pp. 502-514, 2018.
- [2] M. Y. Suberu, M. W. Mustafa, and N. Bashir, "Energy storage systems for renewable energy power sector integration and mitigation of intermittency," *Renewable and Sustainable Energy Reviews*, vol. 35, pp. 499-514, 2014.
- [3] U. Akram, M. Khalid, and S. Shafiq, "An innovative hybrid wind-solar and battery-supercapacitor microgrid system—Development and optimization," *IEEE access*, vol. 5, pp. 25897-25912, 2017.
- [4] T. S. Ustun, C. Ozansoy, and A. Zayegh, "Recent developments in microgrids and example cases around the world—A review," *Renewable and Sustainable Energy Reviews*, vol. 15, no. 8, pp. 4030-4041, 2011.
- [5] M. G. Molina and P. E. Mercado, "Power flow stabilization and control of microgrid with wind generation by superconducting magnetic energy storage," *IEEE Transactions on Power Electronics*, vol. 26, no. 3, pp. 910-922, 2010.
- [6] P. Basak, S. Chowdhury, S. H. nee Dey, and S. Chowdhury, "A literature review on integration of distributed energy resources in the perspective of control, protection and stability of microgrid," *Renewable and Sustainable Energy Reviews*, vol. 16, no. 8, pp. 5545-5556, 2012.
- [7] S. Sinha and S. Chandel, "Improving the reliability of photovoltaic-based hybrid power system with battery storage in low wind locations," *Sustainable Energy Technologies and Assessments*, vol. 19, pp. 146-159, 2017.
- [8] A. Chidurala, T. K. Saha, N. Mithulanathan, and R. C. Bansal, "Harmonic emissions in grid connected PV systems: A case study on a large scale rooftop PV site," in *2014 IEEE PES General Meeting| Conference & Exposition*, 2014: IEEE, pp. 1-5.
- [9] M. Faisal, M. A. Hannan, P. J. Ker, A. Hussain, M. B. Mansor, and F. Blaabjerg, "Review of energy storage system technologies in microgrid applications: Issues and challenges," *Ieee Access*, vol. 6, pp. 35143-35164, 2018.
- [10] U. Datta, A. Kalam, and J. Shi, "The relevance of large-scale battery energy storage (BES) application in providing primary frequency control with increased wind energy penetration," *Journal of Energy Storage*, vol. 23, pp. 9-18, 2019.
- [11] M. E. Farrag, D. M. Hepburn, and B. Garcia, "Quantification of efficiency improvements from integration of battery energy storage systems and renewable energy sources into domestic distribution networks," *Energies*, vol. 12, no. 24, p. 4640, 2019.
- [12] G. Parise, L. Martirano, M. Kermani, and M. Kermani, "Designing a power control strategy in a microgrid using PID/fuzzy controller based on battery energy storage," in *2017 IEEE International Conference on Environment and Electrical Engineering and 2017 IEEE Industrial and Commercial Power Systems Europe (EEEIC/I&CPS Europe)*, 2017: IEEE, pp. 1-5.
- [13] M. A. Ali, "Control of a microgrid through energy storage devices using evolutionary and neuro-fuzzy methods," Master's Thesis, King Fahd University of Petroleum and Minerals Dhahran ..., 2013.
- [14] C. Fu and W. Tan, "Decentralised load frequency control for power systems with communication delays via active disturbance rejection," *IET Generation, Transmission & Distribution*, vol. 12, no. 6, pp. 1397-1403, 2017.
- [15] M.-R. Chen, G.-Q. Zeng, and X.-Q. Xie, "Population extremal optimization-based extended distributed model predictive load frequency control of multi-area interconnected power systems," *Journal of the Franklin Institute*, vol. 355, no. 17, pp. 8266-8295, 2018.
- [16] R. Shankar, K. Chatterjee, and R. Bhushan, "Impact of energy storage system on load frequency control for diverse sources of interconnected power system in deregulated power environment," *International Journal of Electrical Power & Energy Systems*, vol. 79, pp. 11-26, 2016.
- [17] M. N. Dudin, E. E. Frolova, O. V. Protopopova, O. Mamedov, and S. V. Odintsov, "Study of innovative technologies in the energy industry: nontraditional and renewable energy sources," *Entrepreneurship and Sustainability Issues*, vol. 6, no. 4, p. 1704, 2019.
- [18] C. Mu, Y. Tang, and H. He, "Improved sliding mode design for load frequency control of power system integrated an adaptive learning strategy," *IEEE Transactions on Industrial Electronics*, vol. 64, no. 8, pp. 6742-6751, 2017.
- [19] G. Rinaldi, M. Cucuzzella, and A. Ferrara, "Third order sliding mode observer-based approach for distributed optimal load frequency control," *IEEE Control Systems Letters*, vol. 1, no. 2, pp. 215-220, 2017.
- [20] L. A. Wong, V. K. Ramachandaramurthy, S. L. Walker, and J. B. Ekanayake, "Optimal placement and sizing of battery energy storage system considering the duck curve phenomenon," *IEEE Access*, vol. 8, pp. 197236-197248, 2020.
- [21] H. Liu, I. Ndiaye, X. Guo, Y. Jiang, A. Elasser, and M. Yan, "Harmonics and Stability Evaluation of Converter-Interfaced Combined Heat and Power Units," in *2020 IEEE/PES Transmission and Distribution Conference and Exposition (T&D)*, 2020: IEEE, pp. 1-5.
- [22] A. S. Bubshait, A. Mortezaei, M. G. Simoes, and T. D. C. Busarello, "Power quality enhancement for a grid connected wind turbine energy system," *IEEE Transactions on Industry Applications*, vol. 53, no. 3, pp. 2495-2505, 2017.
- [23] A. Elsebaay, M. Ramadan, and M. A. A. Adma, "Studying the effect of non-linear loads harmonics on electric generator power rating selection," *European Scientific Journal*, vol. 13, no. 18, pp. 1857-7881, 2017.
- [24] S. Mekhilef, R. Saidur, and M. Kamalisarvestani, "Effect of dust, humidity and air velocity on efficiency of photovoltaic cells," *Renewable and sustainable energy reviews*, vol. 16, no. 5, pp. 2920-2925, 2012.
- [25] A. Banik, A. Shrivastava, R. M. Potdar, S. K. Jain, S. G. Nagpure, and M. Soni, "Design, modelling, and analysis of novel solar PV system using MATLAB," *Materials today: proceedings*, 2021.
- [26] M. Abdel-Salam, M.-T. El-Mohandes, and M. Goda, "An improved perturb-and-observe based MPPT method for PV systems under varying irradiation levels," *Solar Energy*, vol. 171, pp. 547-561, 2018.
- [27] N. Prabaharan and K. Palanisamy, "Analysis and integration of multilevel inverter configuration with boost converters in a photovoltaic system," *Energy Conversion and Management*, vol. 128, pp. 327-342, 2016.
- [28] B. Lekouaghet, A. Boukabou, N. Lourci, and K. Bedrine, "Control of PV grid connected systems using MPC technique and different inverter configuration models," *Electric Power Systems Research*, vol. 154, pp. 287-298, 2018.
- [29] M. Hannan *et al.*, "Battery energy-storage system: A review of technologies, optimization objectives, constraints, approaches, and outstanding issues," *Journal of Energy Storage*, vol. 42, p. 103023, 2021.
- [30] Y. Li, Z. Yang, D. Zhao, H. Lei, B. Cui, and S. Li, "Incorporating energy storage and user experience in isolated microgrid dispatch using a multi-objective model," *IET Renewable Power Generation*, vol. 13, no. 6, pp. 973-981, 2019.
- [31] B. Mukhopadhyay and D. Das, "Multi-objective dynamic and static reconfiguration with optimized allocation of PV-DG and battery energy storage system," *Renewable and Sustainable Energy Reviews*, vol. 124, p. 109777, 2020.
- [32] A. N. Jog and N. G. Apte, "An adaptive hysteresis band current controlled shunt active power filter," in *2007 Compatibility in Power Electronics*, 2007: IEEE, pp. 1-5.
- [33] B. H. Vaddi Ramesh and M. D. Reddy, "An adaptive hysteresis band current controlled shunt active power filter," *International Journal of Advanced Research in Electrical, Electronics and Instrumentation Engineering*, vol. 3, no. 3, 2014.
- [34] K. Mahboob, S. Tanveer, F. Ali, M.N. Khan, and Q. Awais, "Types and applications of renewable energy technologies and their effect on environment in Pakistan", *Pakistan Journal of Science*, 2019.
- [35] K. Mehboob, "Design and Modeling of tabular receiver of a solar tower power plant," *Pakistan Journal of Enineering and Technolgy*, vol. 4, no. 1, pp. 201-206, 2021.